Integrated 4H-SiC Photosensors With Active Pixel Sensor-Type Circuits for MGy-Class Radiation Hardened CMOS UV Image Sensor

Masayuki Tsutsumi, Tatsuya Meguro, Akinori Takeyama, Takeshi Ohshima, Yasunori Tanaka, and Shin-Ichiro Kuroki, *Member, IEEE*

***Abstract*— For radiation-hardened CMOS image sensor (CIS), 4H-SiC photosensors with active pixel sensor (APS)-type circuits were developed and demonstrated. The dark current of 4H-SiC photodiodes was <2 nA/cm^2. The spectral sensitivity characteristics were also evaluated in the wavelength from 200 nm to 400 nm. The maximal quantum efficiency was 63% at 270 nm. The photosensors with APS type circuits showed high responses to UV light, demonstrating their operation. High gamma-ray dose experiments were also carried out. The dark current after 2 MGy (SiO_2) irradiation was 25 nA/cm^2. The photosensors with APS-type were successfully working after 2 MGy exposure.**

***Index Terms*— 4H-SiC, image sensors, radiation hardened, active pixel sensor, photodiode, MOSFETs, UV.**

I. Introduction

EXPANDING the physical boundary of the application of electronics, allow us to develop new frontiers like space, deep underground, and new industrial applications. For example, radiation hardened electronics has been required for the decommissioning of nuclear power stations, e.g., for the Fukushima Daiichi nuclear power station accident in Japan. So far in the decommissioning, robots have been utilized in the power station, however the available time for the operation is limited by the electronics, particularly image sensors. The radiation hardness of standard Si electronics is 0.2 kGy owing to the total ionization effects on Si MOSFETs [1]. Recently, there are some studies of Radiation-Hardened-By-Design (RHBD), which use an enclosed layout transistor (ELT) or guard ring, thin gate oxide [2], [3], [4], [5]. Using this technique, at Si CMOS image sensor (Si CIS), radiation hardness up to several MGy has been demonstrated [5]. On the other hand, these technologies cannot employ standard and versatile designs, which may result in a lower fill factor, increased pixel size, and increased circuit area.

4H-SiC (Silicon Carbide) is a wide bandgap semiconductor and has excellent properties for harsh environment applications. 4H-SiC has a wide bandgap of 3.26 eV. The carrier density is therefore very low, so we can apply this to high temperature applications. Operation of 4H-SiC bipolar junction transistors (BJTs), junction field effect transistors (JFETs), and metal-oxide-semiconductor transistors (MOSFETs) have been demonstrated in high temperature environments [6], [7], [8], [9]. In addition to this feature, SiC has a higher atomic replacement threshold energy [10], and higher radiation ionization energy [11] than silicon. These properties mean SiC crystal has a hardness to radiation and has potential to realize an electronic device with low soft errors. Radiation-hardened SiC devices have been reported [1], [12], [13]. 4H-SiC BJT and MOSFETs were demonstrated at up to 3.4 MGy [12] and 1.13 MGy [13], respectively. When 4H-SiC is used as a photodetector, ultra violet (UV) light can be accurately detected by this photo detector due to its wide bandgap. Thus, the development of 4H-SiC image sensors has two advantages: they can be adapted to harsh environments such as high temperatures and high radiation, and they can specialize in UV light detection. 4H-SiC has already demonstrated operation as a UV imaging system based on 4H-SiC bipolar transistor [14]. However, if we apply SiC MOSFETs to the pixel device, we can make the device fully planar one, and make the circuits simple ones. In CIS, each pixel has a photodiode (PD), which is a photodetector, and MOSFETs for charge reset and charge amplification. We propose a 4H-SiC CIS as an image sensor for harsh environments.

In this letter, to realize 4H-SiC CIS, 4H-SiC photosensors with active pixel sensor (APS)-type Circuits were fabricated and their radiation hardness was demonstrated by gamma irradiation tests. Our target specifications for imaging are dark current <1 nA/cm^2, dynamic range (DR) > 50 dB, and quantum efficiency (QE) > 60 % [5], [15]. In addition, considering the use in nuclear power plants, the target radiation hardness is >1 MGy.

II. Experimental Details

In this experiment, photosensors with two APS-type circuits, a 3-transistor active pixel sensor (3T-APS)-type and a 4-transistor active pixel sensor (4T-APS)-type, were designed and fabricated. The circuit schematics are shown

Manuscript received 9 November 2022; revised 22 November 2022 and 28 November 2022; accepted 30 November 2022. Date of publication 2 December 2022; date of current version 28 December 2022. This work was supported in part by The Center of World Intelligence Project for Nuclear S&T and Human Resource Development, Strategic Nuclear Power Joint Research Program, under the Ministry of Education, Culture, Sports, Science and Technology (MEXT), Japan, and JSPS KAKENHI (A), under Grant JP20H00252. The review of this letter was arranged by Editor T.-Y. Seong. *(Corresponding author: Shin-Ichiro Kuroki.)*

Masayuki Tsutsumi, Tatsuya Meguro, and Shin-Ichiro Kuroki are with the Research Institute for Nanodevices, Hiroshima University, Hiroshima 739-8527, Japan (e-mail: tsutsumi-masayuki@hiroshima-u.ac.jp; skuroki@hiroshima-u.ac.jp).

Akinori Takeyama and Takeshi Ohshima are with the National Institutes for Quantum Science and Technology (QST), Takasaki 370-1292, Japan.

Yasunori Tanaka is with the National Institute of Advanced Industrial Science and Technology (AIST), Ibaraki 305-8568, Japan.

Color versions of one or more figures in this letter are available at https://doi.org/10.1109/LED.2022.3226494.

Digital Object Identifier 10.1109/LED.2022.3226494

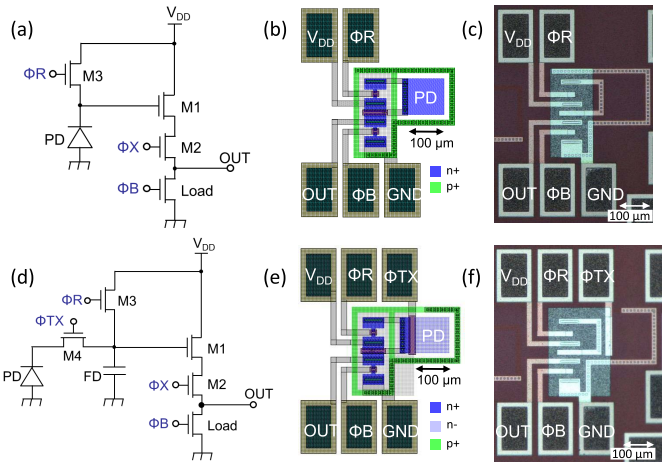

Fig. 1. Photosensors with APS-type circuits:3T-APS-type (a) circuit, (b) layout and (c) micrograph of the fabricated device, 4T-APS-type (d) circuits, (e) layout and (f) micrograph of the fabricated device.

in Fig.1 (a) and (d), respectively. Typically, the 3T-APS-type consists of one photodiode and three MOSFETs. Three MOSFETs serve as reset (M3), source follower (M1), and row selector (M2). On the other hand, the 4T-APS-type has another nMOSFET (M4) for charge transfer between the photodetector and nMOSFETs, resulting in low noise and high sensitivity. The photosensors with APS-type layouts in this experiment are shown in Fig.1 (b), (e). In this devices, the row selector (M2) was not included in the circuit, however a load transistor is added to tune output voltage of the source follower amplifier. At the 4T-APS-type, Simple PD structure was formed, and pinned PD (PPD) with additional p+ layer was not formed. The size of the PD was 100 μm square. Taking into account the capacitance of the prober needles during measurements and the gate overlap capacitance in the process, the nMOSFETs of M1, M3, Load were designed with L/W = 5/60, 5/10, and 5/10 μm, respectively.

The device fabrication process is as follows. A p-type epitaxial layer of 5 μm was grown on SiC bulk substrate. The impurity in the p-epi layer is aluminum (Al) with a concentration of 5.4×10^{16} cm^{-3}. After a first cleaning of the substrate, impurity doping was performed. Since this impurity doping was a high-temperature ion implantation at 500°C, a dummy gate process using a SiO_2 hard mask was employed. Ion implantations were carried out at the n+/n-/p+ regions shown in Fig.1. (b) and (e). The n-, n+, and p+ concentrations are 5.0×10^{17} cm^{-3}, 5.0×10^{19} cm^{-3}, and 5.0×10^{20} cm^{-3}, respectively. These regions formed the PD, the S/D of the nMOSFET, and contact to substrate. Next, after forming the passivation layer by LPCVD, the gate region of the nMOSFETs was etched and dry oxidized. The thickness of the gate oxide film was 22 nm. Then, nickel(Ni)/ niobium(Nb) thin films were deposited, and silicidation were carried out at a temperature of 930 °. After that, interlayer dielectric SiO_2 layer and Al metal wires were formed. The cross-sectional structure of the fabricated device is shown in Fig. 2. As can be seen, the device is a front-side illuminated sensor without a microlens.

Gamma-ray irradiation on the devices was carried out at a cobalt-60 irradiation facility in Japan; the Takasaki Advanced Radiation Research Institute, National Institutes for Quantum Science and Technology (QST). The devices were irradiated with a gamma-ray dose rate of 7.5 kGy/h. The total gamma-ray dose was 2 MGy(SiO_2). During the irradiation, the substrate with the devices was grounded and bias voltage was not applied to all electrodes. The electrical characteristics were measured at room temperature prior to irradiation and after irradiations up to 2 MGy.

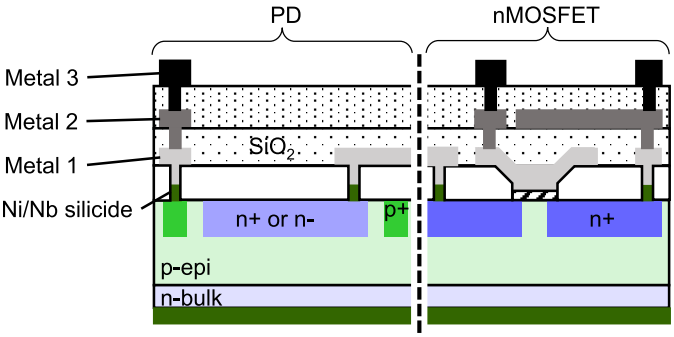

Fig. 2. Cross section of 4H-SiC devices.

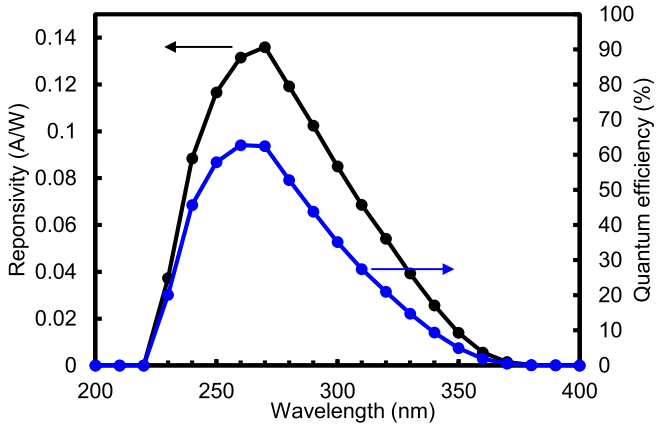

Fig. 3. Responsivity and quantum efficiency of 4H-SiC UV-PDs.

III. Results and Discussion

A. Responsivity and Quantum Efficiency of 4H-SiC PD

In the 4H-SiC PD fabricated on the same chip, reverse current was measured as dark current. The PD dark current before gamma irradiation was <2 nA/cm^2. The responsivity of each wavelength between 200-400 nm was measured with a monochromator (MLS1510 Asahi spectra). The results are shown in Fig. 3. This graph shows the UV photodiode had a sensitivity from a wavelength of 230 nm to 380 nm and took a maximal value at 270 nm. At 270 nm, the responsivity was 0.136 A/W and the quantum efficiency was 63 %. This is sensitive enough for imaging. 4H-SiC has the energy bandgap of 3.26 eV, and the corresponding threshold wavelength of light absorption is 380 nm. The sensitivity threshold of the PD at the longer wavelength side took the same value. Below a wavelength of 250 nm, the absorption coefficient becomes an order of 1.0×10^5 cm^{-1}, and then UV light penetration length becomes a value below 100 nm. The thickness of the n+ region in the PDs was 70 nm, and then at the short wavelength side electron-hole pairs were annihilated easily, and then the responsivity became a lower value.

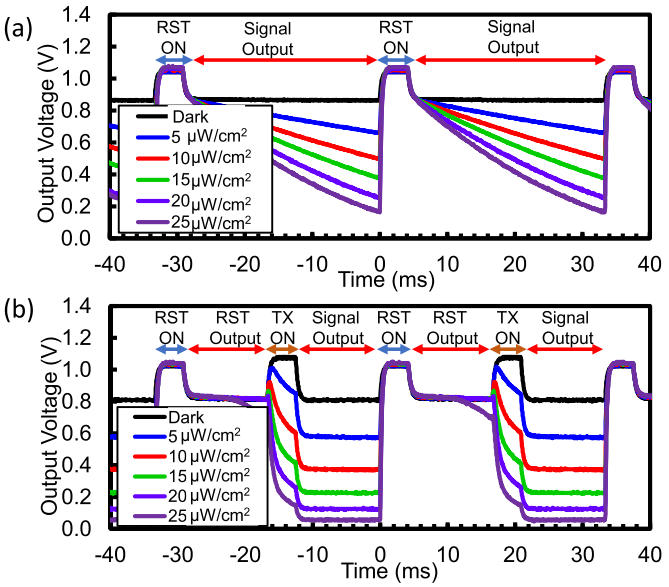

Fig. 4. Output characteristics of fabricated devices: (a) 3T-APS-type and (b) 4T-APS-type (with PD).

B. Photosensors With 3T/4T-APS-Type Circuits

Fig. 4 (a) and (b) shows output characteristics of photosensors with 3T/4T-APS-type circuits. Under UV light irradiation, changes of output voltage were measured. The wavelength of UV light was 320 nm. At the 3T-APS-type, after the reset operation in the dark condition, the output voltage remains constant. By the UV light irradiation, the output voltage decreased, and by increasing the UV power, this amplitude became a higher value. This is because by UV light irradiation, electron-hole pairs are generated at the 4H-SiC PD, and the electrons are stored in PD capacitance. By storing the electrons, the output voltage decreases. At the 4T-APS-type, after the reset operation, by UV light exposure, electrons were stored in the PD, and after the transfer gate was turned on, and the electrons were transferred from the PD to floating diffusion (FD). After the transfer gate was turned off, the output voltage took a constant value, and the value became lower by increasing UV light power.

The relationship between signal voltage and UV power before gamma irradiation is shown in Fig. 5(b). Here, the difference between the voltage values immediately after a reset (V_{RST}) and immediately before the next reset, is the signal voltage (V_{sig}). At both 3T-APS-type and 4T-APS-type, when the UV light exposure time was 29 msec, the dependency showed linearity at below a UV power of 20 μW/cm^2. Above this power, the output voltage was saturated. The DR obtained from the dark current and the photocurrent at the saturation was 62.5 dB. The conversion gains for 3T-APS-type and 4T-APS-type are 0.018 μW/e, 0.021 μW/e, respectively. They are relatively small value compared to 5.7 μV/e, which is the conversion gain of Radiation-Hardened CMOS APS [4]. This is because the size of our fabricated photosensors are very larger than that of them [4], and the capacitance of the PD or FD is large. The larger capacitance makes the voltage swing lower for each collected charge.

C. 2 MGy Radiation Hardness

The output voltage of the 3T-APS-type after 2 MGy irradiation is shown in Fig. 5 (a). The UV responses and charge

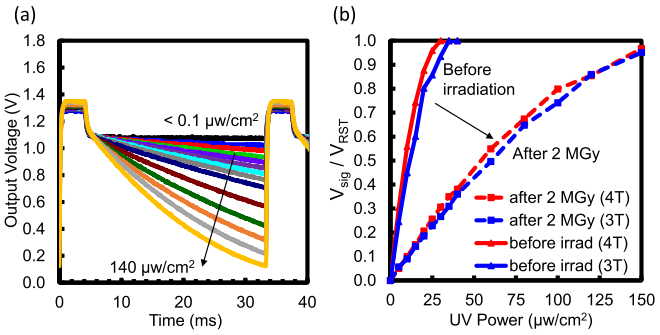

Fig. 5. (a) Output characteristics of photosensor with 3T-APS-type circuits after 2 MGy irradiation. (b) Output signal as a function of UV power ($\lambda = 320$ nm).

resetting were observed as being the same as before irradiation, and this result indicated that the device was working. In addition, the voltage shift in the dark is almost negligible. The dark current after 2 MGy irradiation in 4H-SiC PD was 25 nA/cm^2. The rate of dark current increase of Si PD, which is designed to be hard against radiation, is 1 to 2 pA/cm^2/krad [4]. In comparison, 25nA/cm^2 at 2 MGy is sufficiently low, indicating the radiation hardness of 4H-SiC.

On the other hand, compared to Fig. 4 (a), the entire output waveform is shifted upward. This is related to threshold voltage shift in nMOSFETs due to the total ionizing dose (TID) effect. Fig. 5 (b) shows output voltage as a function of UV power before and after gamma-ray irradiation. The sensitivity to the UV light decreases with increasing TID. However, the output signal after 2 MGy irradiation shows a linear curve to the UV power. Operation was also demonstrated in the 4T-APS-type after irradiation. The above output waveform shift and sensitivity reduction were also confirmed in the 4T-APS-type. No significant leakage current leading to failure was observed, successfully demonstrating the radiation hardness of the 4H-SiC photosensors with APS-type circuits up to 2 MGy.

IV. Conclusion

4H-SiC photosensors with APS-type circuits were fabricated and demonstrated for radiation hardened CIS. 4H-SiC PD spectral response characteristics were evaluated and a maximum quantum efficiency of 63% was obtained at a wavelength of 270 nm. The dark current was <2 nA/cm^2. The photosensors with 3T/4T-APS-type circuits showed a response to UV light and operated. Finally, the fabricated devices were irradiated up to 2 MGy. The dark current was 25 nA/cm^2 after irradiation. Photosensors with 3T/4T-APS-type circuits show a liner output signal to the UV power and were successfully demonstrated.

References

[1] K. K. Lee, T. Ohshima, and H. Itoh, "Performance of gamma irradiated p-channel 6H-SiC MOSFETs: High total dose," *IEEE Trans. Nucl. Sci.*, vol. 50, no. 1, pp. 194–200, Feb. 2003, doi: 10.1109/TNS.2002.807853.

[2] W. Snoeys, F. Faccio, M. Burns, M. Campbell, E. Cantatore, N. Carrer, L. Casagrande, A. Cavagnoli, C. Dachs, S. D. Liberto, F. Formenti, A. Giraldo, E. H. M. Heijne, P. Jarron, M. Letheren, A. Marchioro, P. Martinengo, F. Meddi, B. Mikulec, M. Morando, M. Morel, E. Noah, A. Paccagnella, I. Ropotar, S. Saladino, W. Sansen, F. Santopietro, F. Scarlassara, G. F. Segato, P. M. Signe, F. Soramel, L. Vannucci, and K. Vleugels, "Layout techniques to enhance the radiation tolerance of standard CMOS technologies demonstrated on a pixel detector readout chip," *Nucl. Instrum. Methods Phys. Res. A, Accel. Spectrom. Detect. Assoc. Equip.*, vol. 439, nos. 2–3, pp. 349–360, Jan. 2000, doi: 10.1016/s0168-9002(99)00899-2.

[3] G. Anelli, M. Campbell, M. Delmastro, F. Faccio, S. Florian, A. Giraldo, E. Heijne, P. Jarron, K. Kloukinas, A. Marchioro, P. Moreira, and W. Snoeys, "Radiation tolerant VLSI circuits in standard deep submicron CMOS technologies for the LHC experiments: Practical design aspects," *IEEE Trans. Nucl. Sci.*, vol. 46, no. 6, pp. 1690–1696, Dec. 1999, doi: 10.1109/23.819140.

[4] J. Bogaerts, B. Dierickx, G. Meynants, and D. Uwaerts, "Total dose and displacement damage effects in a radiation-hardened CMOS APS," *IEEE Trans. Electron Devices*, vol. 50, no. 1, pp. 84–90, Jan. 2003, doi: 10.1109/TED.2002.807251.

[5] V. Goiffon, F. Corbiere, S. Rolando, M. Estribeau, P. Magnan, B. Avon, J. Baer, M. Gaillardin, R. Molina, P. Paillet, S. Girard, A. Chabane, P. Cervantes, and C. Marcandella, "Multi-MGy radiation hard CMOS image sensor: Design, characterization and X/gamma rays total ionizing dose tests," *IEEE Trans. Nucl. Sci.*, vol. 62, no. 6, pp. 2956–2964, Dec. 2015, doi: 10.1109/TNS.2015.2490479.

[6] L. Lanni, B. G. Malm, M. Ostling, and C.-M. Zetterling, "500°C bipolar integrated OR/NOR gate in 4H-SiC," *IEEE Electron Device Lett.*, vol. 34, no. 9, pp. 1091–1093, Sep. 2013, doi: 10.1109/LED.2013.2272649.

[7] M. Shakir, S. Hou, B. G. Malm, M. Östling, and C.-M. Zetterling, "A 600 °C TTL-based 11-stage ring oscillator in bipolar silicon carbide technology," *IEEE Electron Device Lett.*, vol. 39, no. 10, pp. 1540–1543, Oct. 2018, doi: 10.1109/LED.2018.2864338.

[8] P. G. Neudeck, L. Chen, R. D. Meredith, D. Lukco, D. J. Spry, L. M. Nakley, and G. W. Hunter, "Operational testing of 4H-SiC JFET ICs for 60 days directly exposed to Venus surface atmospheric conditions," *IEEE Electron Device Lett.*, vol. 39, no. 10, pp. 1540–1543, Oct. 2018, doi: 10.1109/LED.2018.2864338.

[9] V. Van Cuong, S. Ishikawa, T. Maeda, H. Sezaki, T. Meguro, and S.-I. Kuroki, "High-temperature reliability of integrated circuit based on 4H-SiC MOSFET with Ni/Nb ohmic contacts for harsh environment applications," *Jpn. J. Appl. Phys.*, vol. 59, no. 12, Nov. 2020, Art. no. 126504, doi: 10.35848/1347-4065/abc924.

[10] A. L. Barry, B. Lehmann, D. Fritsch, and D. Braunig, "Energy dependence of electron damage and displacement threshold energy in 6H silicon carbide," *IEEE Trans. Nucl. Sci.*, vol. 38, no. 6, pp. 1111–1115, Dec. 1991, doi: 10.1109/23.124082.

[11] C. A. Klein, "Bandgap dependence and related features of radiation ionization energies in semiconductors," *J. App. Phys.*, vol. 39, no. 4, pp. 2029–2038, Mar. 1968, doi: 10.1063/1.1656484.

[12] S. S. Suvanam, S.-I. Kuroki, L. Lanni, R. Hadayati, T. Ohshima, T. Makino, A. Hallen, and C.-M. Zetterling, "High gamma ray tolerance for 4H-SiC bipolar circuits," *IEEE Trans. Nucl. Sci.*, vol. 64, no. 2, pp. 852–858, Feb. 2017, doi: 10.1109/TNS.2016.2642899.

[13] S. Kuroki, H. Nagatsuma, M. de Silva, S. Ishikawa, T. Maeda, H. Sezaki, T. Kikkawa, T. Makino, T. Ohshima, M. Östling, and C. M. Zetterling, "Characterization of 4H-SiC nMOSFETs in harsh environments, high-temperature and high gamma-ray radiation," *Mater. Sci. Forum*, vol. 858, pp. 864–867, May 2016, doi: 10.4028/www.scientific.net/msf.858.864.

[14] S. Hou, M. Shakir, P.-E. Hellstrom, B. G. Malm, C.-M. Zetterling, and M. Ostling, "A silicon carbide 256 pixel UV image sensor array operating at 400 °C," *IEEE J. Electron Devices Soc.*, vol. 8, pp. 116–121, 2020, doi: 10.1109/JEDS.2020.2966680.

[15] D.-L. Lin, C.-C. Wang, and C.-L. Wei, "Quantified temperature effect in a CMOS image sensor," *IEEE Trans. Electron Devices*, vol. 57, no. 2, pp. 422–428, Feb. 2010, doi: 10.1109/TED.2009.2037389.